Bull Math Biol (2012) 74:2165–2182
DOI 10.1007/s11538-012-9751-z

ORIGINAL ARTICLE

A Differential Equation Model of Collagen Accumulation in a Healing Wound

Rebecca A. Segal · Robert F. Diegelmann · Kevin R. Ward · Angela Reynolds

Received: 31 March 2011 / Accepted: 2 July 2012 / Published online: 19 July 2012

Abstract Wound healing is a complex biological process which involves many cell types and biochemical signals and which progresses through multiple, overlapping phases. In this manuscript, we develop a model of collagen accumulation as a marker of wound healing. The mathematical model is a system of ordinary differential equations which tracks fibroblasts, collagen, inflammation and pathogens. The model was validated by comparison to the normal time course of wound healing where appropriate activity for the inflammatory, proliferative and remodeling phases was recorded. Further validation was made by comparison to collagen accumulation experiments by Madden and Peacock (Ann. Surg. 174(3):511–520, 1971). The model was then used to investigate the impact of local oxygen levels on wound healing. Finally, we present a comparison of two wound healing therapies, antibiotics and increased fibroblast proliferation. This model is a step in developing a comprehensive model of wound healing which can be used to develop and test new therapeutic treatments.

R.A. Segal (✉) · A. Reynolds
Department of Mathematics, Virginia Commonwealth University, Richmond, VA 23284-2014, USA
e-mail: rasegal@vcu.edu

R.A. Segal · R.F. Diegelmann
Center for the Study of Biological Complexity, Virginia Commonwealth University, Richmond, VA 23284-2030, USA

R.F. Diegelmann
Department of Biochemistry & Molecular Biology, Virginia Commonwealth University Medical Center, Richmond, VA 23298-0614, USA

R.F. Diegelmann · A. Reynolds
VCURES, Virginia Commonwealth University, Richmond, VA 23298, USA

K.R. Ward
Michigan Critical Injury and Illness Research Center, Department of Emergency Medicine, University of Michigan, Ann Arbor, MI 48109, USA

Keywords Acute wound · Collagen · Mathematical modeling · Computational modeling

1 Introduction

The care of acute and chronic wounds is a source of significant health care cost. Diabetes, in particular, often leads to chronic wounds that require care for the life of the patient. It has been estimated that the cost of treating chronic wounds is $5–$10 billion a year (Kuehn 2007). Additionally, patients sustaining polytrauma often have complications from wounds, which can secondarily lead to sepsis, multi-organ failure and death.

The process undertaken by the human body to close a wound is complex. There are four stages to the wound healing process (Goldberg and Diegelmann 2010), each of which is subject to derailment and is a potential cause for failure in satisfactory wound closure. The four stages of wound healing are hemostasis, inflammation, proliferation, and remodeling. The stages overlap in time and each involve many different biochemical processes and cell types. An understanding of the interplay between the key mediators from each stage will lead to a greater understanding of the wound healing process.

In recent years, there has been an effort to use mathematical modeling to help understand the complexities involved in wound healing. A review of recent modeling efforts in the area of wound healing (Sherratt and Dallon 2002) addresses the different aspects of wound healing and outlines many of the modeling techniques relevant to the field. Because wound healing involves so many biological processes, there have been many different types of modeling technique used. Some research is concerned with the geometry of the wound and focused on the formation of the skin matrix (Almeida et al. 2011; Javierre et al. 2009). These models do not implement the effect of inflammation, an important stage of wound healing, particularly for wounds that fail to heal. Other research has been focused on the question of tissue oxygenation and how supplementation or reduction of oxygen impacts the wound healing process (Friedman et al. 2010; Flegg et al. 2010). Because of the geometric nature of angiogenesis, these models are implemented with partial differential equations and are computationally expensive. Finally, there is research focused on the biochemical processes involved in the regulation of the wound healing process (Menke et al. 2010; Reynolds et al. 2006). Our model builds on the research in this area by adding further complexities to these existing models.

2 Model Development

This model aims to capture the dynamics of healing tissue by monitoring collagen accumulation in a wound. Collagen is the major protein component of the wound matrix and serves as a useful marker because it can be measured during the healing process. Additionally, changes in collagen production during the phases of wound healing are well correlated with actual healing. Collagen is produced by fibroblast

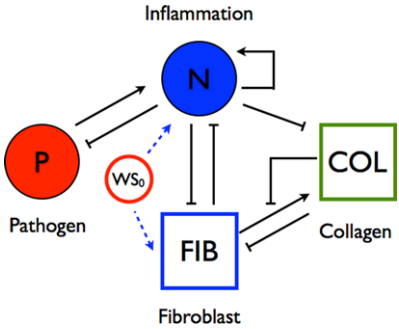

Fig. 1 Model schematic for collagen accumulation model where WS_0 is the initial wound size. The creation of a wound triggers the recruitment of fibroblast from the healthy tissue at the edge of the wound as well as the inflammatory response, *dashed arrows*. The fibroblasts proliferate and migrate. *Arrows* represent up regulation, while *bars* represent down regulation and/or inhibition

cells, one of the major cell types involved in wound healing. The differential equation model tracks changes in the amount of pathogens, inflammatory cells, collagen and the different stages of fibroblasts. Wound size is also tracked, as a direct function of the collagen deposition.

Figure 1 depicts the relationship between the cell types. An initial wound event (WS_0) triggers an inflammatory response. An additional inflammatory response may be induced by the introduction of pathogens (P) into the wound. There are many different inflammatory cell types and mediators which may be activated and produced during the wound healing process. These are not explicitly modeled, but are grouped together and are represented with the variable N. The activated inflammatory cells, along with their byproducts, cause further tissue damage by destroying fibroblasts (FIB) as well as the newly formed collagen (COL).

2.1 Variables and Parameters

The model contains a large number of parameter values (Table 1). The values for many of these parameters were taken from Reynolds et al. (2006). The units for the model variables and associated parameters are non-specific because they represent the combination of various cells, signaling proteins and mediators. Therefore, most of the variables represent a relative level of response, rather than an exact cell count. The variable COL represents a percentage of space filled by collagen and is therefore dimensionless. The variable P represents the concentration of pathogen cells within the wound. The remaining parameter values in the table were estimated using the known time course for normal wound healing and then confirmed using the collagen accumulation data (Madden and Peacock 1971).

2.2 Fibroblast Equations

The fibroblast population is divided into three different groups depending on the cell's primary activity. Fibroblasts are recruited to the wound site after the initial wound insult in response to the inflammatory activity (Diegelmann and Evans 2004). These

Table 1 Parameter values for collagen accumulation model

Name	Description	Baseline value
μ_{fib}	Decay rate of the fibroblasts	0.1/day
$p_{\text{fib}x}$	Proliferation rate of FIB_x	m: 0.6, p: 0.4, a: 0.3/day
d_{f}	Transition rate of the FIB_x	0.3/day
$k_{\text{fn}x}$	The rate at which N destroys FIB_x	m: 0.5, p: 0.4, a: 0.3/day
x_{fn}	The Hill constant for the destruction of fibroblasts by N	0.6 N-units
p_{bl}	Baseline proliferation becomes nonzero when $COL \cdot FIB > 0.01$	0.08 F-units/day
k_{cf}	The rate at which FIB_{a} produces COL	1/day
x_{cf}	The Hill constant for the production of COL by FIB_a	4.2 F-units
h_{fc}	The inhibition exponent for contact inhibition in COL production term	1
k_{cn}	The rate at which N destroys COL	2/N-units/day
k_{cfr}	The rate at which FIB_{a} degrades COL	500/day
x_{cfr}	The Hill constant for degradation of COL by FIB_{a}	5 F-units
N_{crit}	Threshold below which N must fall before the wound can enter the remodeling stage	0.01 N-units
k_{np}	Rate at which P activates N	0.5/P-units/day
k_{nn}	Rate at which the immune mediators activate N	$3/\text{N}^3$-units/day
k_{nw}	Rate at which the wound (WS) activates N	2/day
s_{nr}	Source rate for resting inflammatory cells	2N-units/day[a]
μ_{nr}	Decay rate of resting inflammatory cells	2.88/day[a]
k_{nf}	Rate at which FIB_{a} destroys N	0.1/F-units/day
μ_{n}	Decay rate of N	1.2/day[a]
n_{∞}	The inhibition constant for the inhibition of FIB_x proliferation/transition by N.	0.6 N-units
c_{∞}	The inhibition constant for contact inhibition of FIB_x proliferation by collagen (COL)	0.5
h_{c}	The inhibition exponent for contact inhibition of FIB_x proliferation by collagen (COL)	4
$c_{\text{f}\infty}$	The inhibition constant for contact inhibition in COL production term	0.8 COL-units
$c_{\text{fr}\infty}$	The inhibition constant for contact inhibition in COL degradation tem	1.8 COL-units
F_{∞}	The inhibition constant for the inhibition of inflammation N by active fibroblast FIB_a	6 F-units
P_{∞}	Maximum of the pathogen population	20×10^6/cc[a]
k_{pg0}	Pathogen growth rate when O_2 is at its normal level	0.55/day[a]
β_{p}	Maximum increase in the growth rate of pathogen possible due to reduction in O_2 levels	0.3/day
O_{crit}	Normal O_2 level	25
k_{pm}	Rate at which M destroys pathogen P	0.6/M-units/day
s_{m}	Source of background immune mediators M. These are initially present at the wound.	0.12/M-units/day[a]
μ_{m}	Decay rate of M	0.048/day[a]
k_{mp}	Rate at which M is activated by P	0.108/P-units/day
k_{pn}	Rate at which inflammation N destroys P	0.2/N-units/day
w_{sg}	Determines how altered O_2 level determine effective wound size	0.6

[a]Parameters determined from Reynolds et al. (2006)

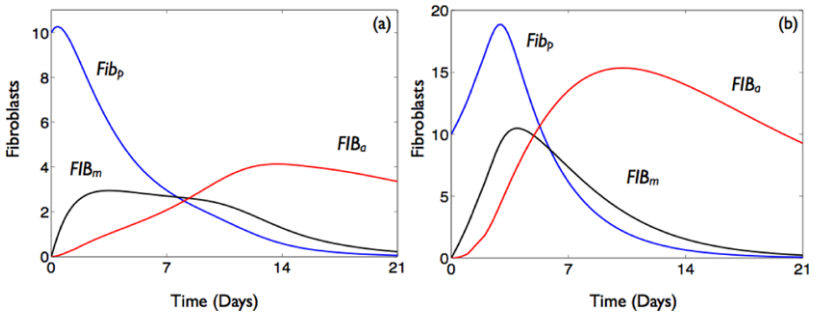

Fig. 2 Fibroblast stages during wound healing with and without an inflammatory response. Transients for proliferating fibroblasts (FIB_{p}), migrating fibroblasts (FIB_{m}) and active fibroblasts (FIB_{a}) with $WS_0 = 0.6$. All other variables were initially set to background levels, $COL = 0$, $N = 0$, $FIB_{\mathrm{p}} = 10$, $FIB_{\mathrm{m}} = 0$, and $FIB_{\mathrm{a}} = 0$. (**a**) Shows activity with a normal inflammatory response. (**b**) Shows activity with inflammatory response suppressed

cells then progress through three stages of activity. They proliferate (FIB_{p}), then they migrate further into the wound (FIB_{m}) and, once in place, they become activated and produce collagen (FIB_{a}). In each case, we model the relative activity of cells, not an actual cell count.

Each stage of fibroblast activity is modeled by a separate differential equation. However, all stages of fibroblasts have some basic dynamics in common. Fibroblasts have an intrinsic death rate and a proliferation rate which are proportional to the cell activity, $-\mu_{\mathrm{fib}} FIB_x$ and $p_{\mathrm{fib}x} FIB_x$, respectively. In addition, each stage of fibroblast is negatively impacted by the presence of inflammation. Activated inflammatory cells destroy fibroblast cells (Diegelmann and Evans 2004), as well as hinders the fibroblasts' function at a rate proportional to both the current fibroblast population and a Hill function of N, $-k_{\mathrm{fn}x} f_{\mathrm{H}}(N, x_{\mathrm{fn}}) FIB_x$. The Hill function is of the form $f_{\mathrm{H}}(x, V) = \frac{x}{V+x}$. This function is used to capture the fact that the ability of the inflammatory cells to destroy the fibroblast has maximum rate, $k_{\mathrm{fn}x}$, for each of the fibroblast populations.

In normal skin there is a background level of resident fibroblasts, which are available to be recruited from the surrounding tissue and migrate into the wound from its less damaged outer margins immediately after the wounding event. These fibroblasts exist in both pre-wounded tissue and in healed tissue. Therefore, an initial condition of $FIB_{\mathrm{p}} = 10$ is used to represent the initial availability of proliferating fibroblasts in the surrounding healthy tissue at the margin of the wound following the wounding event. A diffusion type term is used to model the transition from one stage of fibroblast to the next, $-d_{\mathrm{f}} FIB_x$.

Figure 2 shows the relative size and time scale for the influx of the different fibroblast stages with and without inhibition by inflammation. In both panels $FIB_{\mathrm{p}} = 10$ at the start of the simulation. Explicitly modeling the three stages of fibroblasts allows for a slower onset of collagen production in the model without using a delay function. Notice in Fig. 2a that with inflammation FIB_{a} does not reach ten percent of its maximum until approximately 2.2 days, allowing for a delay between the wound event and the availability of FIB_{a} for synthesizing collagen.

The newly synthesized collagen is structurally weaker than native collagen. Fibroblasts continue to respond to the presence of this weaker new collagen. Activated fibroblasts remain at the wound site after the wound has healed (Goldberg and Diegelmann 2010). Therefore, the activated fibroblast (FIB_a) concentration remains nonzero even in a closed wound. To capture this dynamic, we include a source term, p_{bl}, in the (FIB_a) equation. The p_{bl} term becomes nonzero once significant levels of new collagen are present. The above dynamics leads to Eqs. (1)–(3):

$$\frac{dFIB_p}{dt} = -\mu_{fib}FIB_p + p_{fibp}FIB_p - d_fFIB_p - k_{fnp}f_H(N, x_{fn})FIB_p \quad (1)$$

$$\frac{dFIB_m}{dt} = -\mu_{fib}FIB_m + p_{fibm}FIB_m - d_fFIB_m + d_fFIB_p - k_{fnm}f_H(N, x_{fn})FIB_m \quad (2)$$

$$\frac{dFIB_a}{dt} = -\mu_{fib}FIB_a + p_{fiba}FIB_a + d_fFIB_m - k_{fna}f_H(N, x_{fn})FIB_a + p_{bl} \quad (3)$$

with $f_H(x, V) = \frac{x}{V+x}$.

2.3 Collagen Equation

Collagen is synthesized by activated fibroblasts. Once the fibroblasts have proliferated to sufficient levels and have migrated to the appropriate location, they will begin producing collagen fibers, which is modeled with a nonlinear Hill-type term $k_{cf}f_H(FIB_a, x_{cf})$.

When inflammatory cells are present, they release enzymes that can degrade the collagen fibers, and this activity is represented by a mass action term, $-k_{cn}NCOL$. After the tissue has been injured, fibroblasts continue to produce collagen for the life of the tissue (Schilling 1968; Ross 1968). This would lead to excessive scarring, so in the absence of inflammation (i.e., once the wound has healed), fibroblasts also degrade the collagen, $-k_{cfr}f_H(FIB_a, x_{cfr})s_h(N_{crit} - N)$. A smooth approximation of the Heaviside function, s_h, is used, so that this term has an effect only when N is sufficiently low. Once inflammation drops below N_{crit}, $s_h(N_{crit} - N)$ will be one and the term will have an effect on collagen accumulation. The effects of contact inhibition, which will be discussed and included later, control this degradation term in the early stages of healing when N is increasing from zero and has not reached N_{crit}. This dual activity of fibroblasts characterizes the stage of wound healing known as remodeling (Goldberg and Diegelmann 2010). Combining all these dynamics we derive the collagen equation, Eq. (4):

$$\frac{dCOL}{dt} = k_{cf}f_H(FIB_a, x_{cf}) - k_{cn}NCOL - k_{cfr}f_H(FIB_a, x_{cfr})s_h(N_{crit} - N) \quad (4)$$

with $s_h(x) = \frac{1}{1+e^{-50x}}$.

Figure 3 shows the typical time scale for entering into remodeling for a small, uninfected wound by plotting the rate of degradation and production of COL by FIB_a. The production and degradation curves are plots of $k_{cf}f_H(FIB_a, x_{cf})$ and $-k_{cfr}f_H(FIB_a, x_{cfr})s_h(N_{crit} - N)$ respectively, during normal wound healing. The rate of degradation is zero until the inflammation in the wound is eliminated. A balance between degradation and production is quickly met once inflammation is eliminated, but active fibroblasts never return to zero.

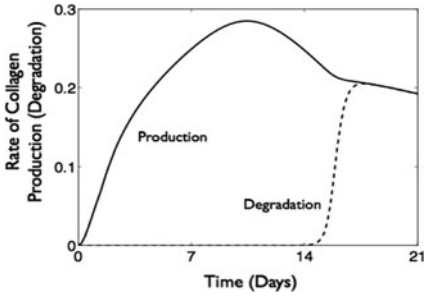

Fig. 3 Remodeling Stage. Rate of collagen production ($k_{\mathrm{cf}} f_{\mathrm{H}}(FIB_{\mathrm{a}}, x_{\mathrm{cf}}, h_{\mathrm{f}})$) and collagen degradation ($-k_{\mathrm{cfr}} f_{\mathrm{H}}(FIB_{\mathrm{a}}, x_{\mathrm{cfr}}, h_{\mathrm{fr}}) \times s_{\mathrm{h}}(N_{\mathrm{crit}} - N)$) by FIB_{a} during wound healing with $WS_0 = 0.6$. All other variables were initially set to background levels, $COL = 0$, $N = 0$, $FIB_{\mathrm{p}} = 10$, $FIB_{\mathrm{m}} = 0$, and $FIB_{\mathrm{a}} = 0$

2.4 Inflammation Equation

The inflammatory response is complex. Previously, Reynolds et al. (2006) derived a detailed model of an acute inflammatory response. This is the type of response that is important in an acute wound. The inflammation equation developed below builds on this previous work which is summarized and expanded upon. Resting inflammatory cells are recruited to the wound site by pathogens, damaged tissue, and other inflammatory cells and mediators (Martin and Leibovich 2005; Eming et al. 2000). Since N represents all activated inflammatory cells and associated mediators collectively, a term for the activation of N from resting inflammatory cells is a function of multiple variables. This activation is triggered by the size of the wound (WS), the amount of pathogen in the wound (P) and the amount of pro-inflammatory mediators produced by inflammatory cells (Diegelmann and Evans 2004). These mediators are not explicitly accounted for: instead, the model uses the level of activated inflammation (N) as a measure of aggregate inflammatory mediator levels. Therefore, activation is dependent on three variables N, WS, and P giving a rate of activation of $R = k_{\mathrm{np}} P + k_{\mathrm{nn}} N^3 + k_{\mathrm{nw}} WS$. An exponent of three on the pro-inflammatory variable is used to account for the accumulation of pro-inflammatory cytokines needed to sustain a positive feedback loop within the pro-inflammatory response. Low levels of N will not cause significant levels of activation, but once N accumulates it can sustain activation of inflammatory cells and the resulting production of pro-inflammatory cytokines. The process of activation occurs on a faster time scale than the other interactions included in this model, and this eliminates the need to explicitly track the resting population of inflammatory cells. A quasi-steady state assumption on the resting population is used and this simplifies the activation process to a single term, $\frac{s_{\mathrm{nr}} R}{\mu_{\mathrm{nr}} + R}$. Further details on the derivation of this type of term are in Reynolds et al. (2006). Because R is dependent on N there is a positive feedback loop that promotes sustained inflammation. This process is controlled during wound healing by inhibition, which is derived later.

Fibroblasts are recruited to the wound site by mediators released from the inflammatory cells and are then able to repair tissue damage and modulate the inflammatory response (Diegelmann and Evans 2004; Menke et al. 2006; Grinnell 1994; Buckley et al. 2001; Smith et al. 1997). This modulation of the inflammatory response is represented with the mass action term, $-k_{\mathrm{nf}} FIB_{\mathrm{a}} N$. The inflammatory cell population will decrease at a greater rate when fibroblasts levels are higher.

Furthermore, there is an intrinsic decay of the inflammatory cells $-\mu_n N$ based on their half-life (Harley et al. 1990; Greenhalgh 1998). Combining all of these dynamics the equation for inflammation is formed, Eq. (5):

$$\frac{dN}{dt} = \frac{s_{nr} R}{\mu_{nr} + R} - k_{nf} FIB_a N - \mu_n N \tag{5}$$

2.5 Inhibition

Equations (1)–(5) are derived above without modeling inhibition of the cellular processes. To more accurately model the cellular and biochemical activity, inhibition must be included. Many of the variables included in this model inhibit each other using various mechanisms. In general, inhibition has been grouped into two types. The first is cell-mediated inhibition modeled by a Hill-type inhibition function, f_i, which is dependent on the cell type being inhibited, x, and cell type causing the inhibition, V, and is of the form $f_i(x, V, V_\infty) = \frac{x}{1+(V/V_\infty)^2}$. The second type, contact inhibition, is modeled as a function of collagen accumulation. As collagen increases, filling the wound, contact inhibition between the cells and the collagen matrix down regulates wound healing activity. Again this nonlinear process is modeled with a Hill-type inhibition function. This function, which has the general form, $f_c(COL, c, h) = \frac{1}{1+(COL/c)^h}$, is always dependent on collagen and is used as a multiplier in terms which are affected by contact inhibition.

Fibroblast proliferation and stage transition are both inhibited by inflammation. In the presence of high inflammation, fibroblasts are limited in their ability to proliferate and migrate (Martin and Leibovich 2005). Therefore, all of the proliferation and stage transition terms in FIB_x are replaced with $f_i(FIB_x, N, n_\infty)$. It is assumed that the level of inhibition due to inflammation is independent of the stage the fibroblast is in and there is no current experimental data to refute this assumption.

Fibroblast activity is down regulated by the filling in of the collagen matrix due to contact inhibition (Takai et al. 2008). Therefore, fibroblast proliferation rates will slow in the presence of collagen fibers. As the wound fills in, there is less need for new fibroblasts. It is also assumed that the level of contact inhibition is independent of the stage the fibroblast is in, so each proliferation term is multiplied by $f_c(COL, c_\infty, 4)$.

Both the production and degradation of collagen are also subject to contact inhibition. Production of new collagen decreases as COL reaches 100 %, because the wound is filling in. The production of collagen by fibroblasts is down regulated as COL increases. This is captured mathematically by having the COL production term multiplied by $f_c(COL, c_{f\infty}, 1)$. Degradation works in the opposite manner. Thus, when collagen levels are high, fibroblasts in the degradation term have less inhibition. Therefore, the multiplier on the COL degradation term is $(1 - f_c(COL, c_{fr\infty}, 12))$.

Fibroblasts inhibit the activation of inflammatory cells (Buckley et al. 2001). This inhibition is accounted for by replacing the basic activation rate with an inhibited activation rate $R_i = f_i(k_{np} P + k_{nn} N^3 + k_{nw} WS, FIB_a, F_\infty)$. That is, when there is high fibroblast activity, the activation of inflammation is suppressed. Once sufficient fibroblasts have been activated and have begun producing collagen, the inflammatory response becomes inhibited, allowing the wound to heal. F_∞ is determined based on

the maximum value achieve by FIB_a in a normal healing wound, such that the timing of the down regulation of inflammation is appropriate.

A full version of the model, with all the inhibition included in each equation, is presented at the end of this section.

2.6 Pathogen Equation

Pathogen growth is modeled with a logistic equation, with a growth rate of $k_{pg}(O_2)$ and a carrying capacity of P_∞. Because the anaerobic pathogen population is increased in low oxygen environments (Kühne et al. 1985), the pathogen growth rate is a function of the oxygen level in the local environment and is determined by the function $k_{pg}(O_2)$, Eq. (6):

$$k_{pg}(O_2) = \begin{cases} k_{pg0}, & \text{if } O_2 \geq O_{crit} \\ k_{pg0} + \beta_p(1 - \frac{O_2}{O_{crit}}), & \text{if } O_2 < O_{crit} \end{cases} \tag{6}$$

This relationship between tissue oxygenation levels and bacterial growth is illustrated in Fig. 4a with O_{crit} set to 25, which was chosen to represent a normal transcutaneous oxygen level of 25 mm Hg (Ballard et al. 1995; Caselli et al. 2005). When the tissue oxygen level is above the critical value, k_{pg0} remains fixed at 0.55.

The second term in Eq. (7) is directly from the Reynolds et al. model and accounts for local immune mediators that immediately interact with the pathogen, such as defensing and non-specific antibodies (Stefanini et al. 2008; Paulsen et al. 2002; Raj and Dentino 2002).

Inflammatory cells such as neutrophils and macrophages actively seek out and remove pathogens from the wound site. These phagocytic cells are less able to migrate in a low oxygen environment (Turner et al. 1999). To account for these dynamics it is assumed that the destruction term for pathogens, $-k_{pn}NP$, is modified by $(1 - g(O_2))$ to model the dependence on O_2 levels. Despite high levels of inflammatory cells in the wound region, the hypoxic environment will impede their ability to reach the pathogens. The function $(1 - g(O_2))$ (Fig. 4b) is designed to capture the decreased effectiveness of cells in a hypoxic environment and to represent better than normal function when O_2 is larger than the critical value, O_{crit}. In Eq. (7),

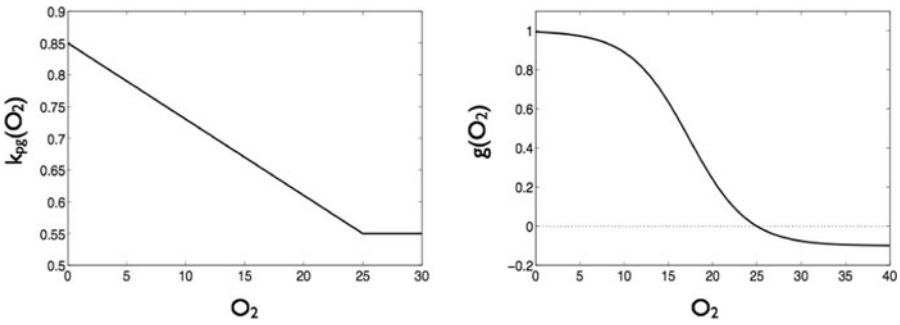

Fig. 4 Auxiliary functions for oxygen. $k_{pg}(O_2)$ and $g(O_2)$. Plots of the functions used to implement the effects of altering local tissue O_2 above or below $O_{crit} = 25$

$(1 - g(O_2))$ is used to modify the ability of inflammatory cells to remove pathogens from the wound. Furthermore, the activity of the inflammatory cells is inhibited by the presence of active fibroblasts, so N was replaced with $f_i(N, FIB_a, F_\infty)$. This nonlinear inhibition of N has FIB_a as the inhibitor with F_∞ controlling the effectiveness of FIB_a as described above. By combining the above terms, the pathogen equation is formed, Eq. (7):

$$\frac{dP}{dt} = k_{pg}(O_2)P\left(1 - \frac{P}{P_\infty}\right) - \frac{k_{pm}s_m P}{\mu_m + k_{mp}P} - k_{pn}Pf_i(N, FIB_a, F_\infty)\big(1 - g(O_2)\big) \tag{7}$$

where $g(V) = 1 - \frac{1.1}{1+0.1e^{-0.3(V-O_{crit})}}$.

2.7 Wound size

Wound closure is a direct result of the production of collagen fibers. These fibers form the matrix that will lead to contraction and closure of the wound. To describe wound closure, the model has a dimensionless variable which measures the effective size of the wound, WS. This is a function of both COL and O_2, Eq. (8). The wound size is prevented from becoming negative by using the max function. This is necessary because the variable COL is allowed to take on values above one in order to account for scarring (due to excess collagen production and abnormal remodeling). The effective wound size accounts for the additional tissue damage which occur in a low oxygen environment. WS is used to determine the rate of activation for N in R_i in Eq. (13). The wound is not considered to be larger in the low oxygen environment, but the byproducts of tissue damage that signal activation are greater. Therefore, WS is interpreted as the effective wound size because it accounts for the effects of reduced O_2 by including the multiplier, $\frac{1}{1-w_{sg}g(O_2)}$:

$$WS = \max\left((1 - COL)WS_0\frac{1}{1 - w_{sg}g(O_2)}, 0\right) \tag{8}$$

2.8 Full Model

Combining all of the equations with inhibition the following system of equations evolves, Eq. (9)–(15):

$$\frac{dFIB_p}{dt} = -\mu_{fib}FIB_p + p_{fibp}f_i(FIB_p, N, n_\infty)f_c(COL, c_\infty, 4) - d_f f_i(FIB_p, N, n_\infty) - k_{fnp}f_H(N, x_{fn})FIB_p \tag{9}$$

$$\frac{dFIB_m}{dt} = -\mu_{fib}FIB_m + p_{fibm}f_i(FIB_m, N, n_\infty)f_c(COL, c_\infty, 4) - d_f f_i(FIB_m, N, n_\infty) + d_f f_i(FIB_p, N, n_\infty) - k_{fnm}f_H(N, x_{fn})FIB_m \tag{10}$$

$$\frac{dFIB_a}{dt} = -\mu_{fib}FIB_a + p_{fiba}f_i(FIB_a, N, n_\infty)f_c(COL, c_\infty, 4) + d_f f_i(FIB_m, N, n_\infty) - k_{fna}f_H(N, x_{fn})FIB_a + p_{bl} \tag{11}$$

$$\frac{dCOL}{dt} = k_{\mathrm{cf}} f_{\mathrm{H}}(FIB_{\mathrm{a}}, x_{\mathrm{cf}}) f_{\mathrm{c}}(COL, c_{\mathrm{f}\infty}, h_{\mathrm{fc}}) - k_{\mathrm{cn}} N COL$$
$$- k_{\mathrm{cfr}} f_{\mathrm{H}}(FIB_{\mathrm{a}}, x_{\mathrm{cfr}}) s_{\mathrm{h}}(N_{\mathrm{crit}} - N)\big(1 - f_{\mathrm{c}}(COL, c_{\mathrm{fr}\infty}, 12)\big) \tag{12}$$

$$\frac{dN}{dt} = \frac{s_{\mathrm{nr}} R_{\mathrm{i}}}{\mu_{\mathrm{nr}} + R_{\mathrm{i}}} - k_{\mathrm{nf}} FIB_{\mathrm{a}} N - \mu_{\mathrm{n}} N \tag{13}$$

$$\frac{dP}{dt} = k_{\mathrm{pg}}(\mathrm{O}_2) P\left(1 - \frac{P}{P_\infty}\right) - \frac{k_{\mathrm{pm}} s_{\mathrm{m}} P}{\mu_{\mathrm{m}} + k_{\mathrm{mp}} P}$$
$$- k_{\mathrm{pn}} P f_{\mathrm{i}}(N, FIB_{\mathrm{a}}, F_\infty)\big(1 - g(\mathrm{O}_2)\big) \tag{14}$$

$$WS = \max\left((1 - COL) WS_0 \frac{1}{1 - w_{\mathrm{sg}} g(\mathrm{O}_2)}, 0\right) \tag{15}$$

where

$$f_{\mathrm{H}}(x, V) = \frac{x}{V + x}$$

$$s_{\mathrm{h}}(x) = \frac{1}{1 + e^{-50x}}$$

$$f_{\mathrm{i}}(x, V, V_\infty) = \frac{x}{1 + (V/V_\infty)^2}$$

$$f_{\mathrm{c}}(COL, c_\infty, h_\infty) = \frac{1}{1 + (COL/c_\infty)^{h_\infty}}$$

$$R_{\mathrm{i}} = f_{\mathrm{i}}\big(k_{\mathrm{np}} P + k_{\mathrm{nn}} N^3 + k_{\mathrm{nw}} WS, FIB, F_\infty\big)$$

$$k_{\mathrm{pg}}(\mathrm{O}_2) = \begin{cases} k_{\mathrm{pg0}}, & \text{if } \mathrm{O}_2 \geq \mathrm{O}_{\mathrm{crit}} \\ k_{\mathrm{pg0}} + \beta_{\mathrm{p}}(1 - \frac{\mathrm{O}_2}{\mathrm{O}_{\mathrm{crit}}}), & \text{if } \mathrm{O}_2 < \mathrm{O}_{\mathrm{crit}} \end{cases}$$

and

$$g(V) = 1 - \frac{1.1}{1 + 0.1 e^{-0.3(V - \mathrm{O}_{\mathrm{crit}})}}$$

3 Results

Using the ODE model, Eqs. (9)–(15), with the baseline parameters in Table 1, a normally healing wound is simulated. This wound was simulated using an initial wound size of $WS_0 = 0.6$, see Fig. 5. The three panels of Fig. 5 show the transients for activated fibroblasts (FIB_{a}), inflammation (N) and collagen (COL). The wound filled with new collagen on approximately the 14th day of healing and inflammation completely subsided within the next two days. Fibroblast activity is sustained after the wound has closed as a result of the wound entering the remodeling stage of wound healing.

When the initial wound size is increased, a chronic wound that is incapable of healing is simulated, see Fig. 6. The initial wound size was increased to 0.8 which resulted in an increased inflammatory response. The maximum of the inflammatory response in the first 3 weeks in Fig. 6 (large wound) is near 0.8 whereas the maximum in Fig. 5 (small wound) is around 0.5. Notice that the fibroblast and collagen levels are

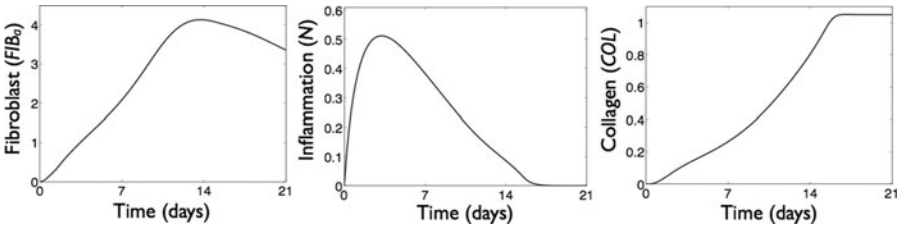

Fig. 5 Transients for normal healing. This wound was created by setting $WS_0 = 0.6$ with all model variables initially set to background levels, $COL = 0$, $N = 0$, $FIB_p = 10$, $FIB_m = 0$, and $FIB_a = 0$

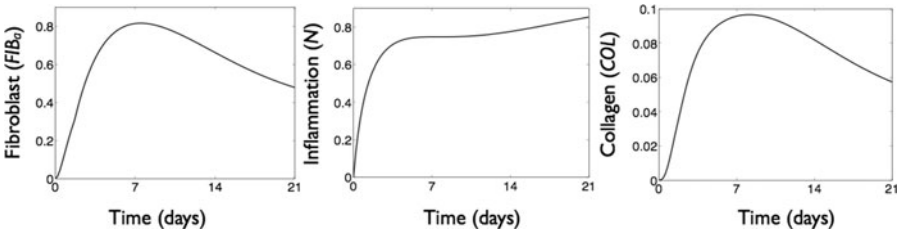

Fig. 6 Transients for a chronic wound. This wound was created by setting $WS_0 = 0.8$ with all model variables initially set to background levels, $COL = 0$, $N = 0$, $FIB_p = 10$, $FIB_m = 0$, and $FIB_a = 0$

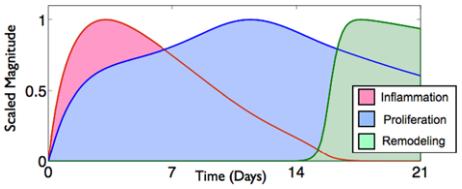

Fig. 7 Stages of wound healing. Transients are plotted for scaled N (*red*—inflammation), the sum of FIB_m and FIB_a (*blue*—proliferation) and collagen degradation term from Eq. (12) (*green*—remodeling). Each transient was scaled by the maximum of the variable model for comparison (Color figure online)

suppressed as a result of the high levels of inflammation and large initial wound size. High levels of inflammation, separate from that produced by infection, can be the result of the large amount of tissue destruction during the initial wounding event. In both of the above cases, no infection was introduced so P remained zero throughout the simulations.

Once the baseline parameters were determined based on achieving the proper time course of healing in a moderate wound, the modeling dynamics were validated by plotting the time course for the stages of wounding healing included in the model, inflammation, proliferation, and remodeling. To illustrate these stages using model variables we plotted N (inflammation), the sum of FIB_m and FIB_a (proliferation), and the degradation term from the collagen equation (remodeling) in Fig. 7. The sum of the FIB_m and FIB_a variables were used, because these two stages represent the fibroblasts that are within the wound and lead to the closing of the wound. The degradation term from the collagen equation is zero outside of the remodeling stage

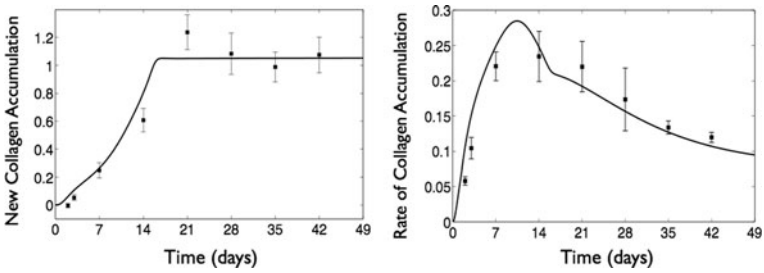

Fig. 8 Comparison of model simulations and experimental data during normal wound healing. Data from Madden and Peacock (1971). $WS_0 = 0.6$ with pathogen, inflammation and fibroblast all initially zero. In the left panel, data were scaled as described in the text so that they represented the same quantity as *COL*. In the *right panel* they were scaled to represent the same quantity as the production term from Eq. (12)

of healing and so it is a good marker for when the remodeling phase has begun. FIB_a does not degrade collagen until the wound has closed. Each of these three stages was scaled so that their maximums were one, in order to easily compare their time courses. Figure 7 shows that the initial days of wound healing is dominated by inflammation and the initiation of fibroblast activity. Inflammation then starts to decrease, moving the wound into the proliferation phase. In the final stage, inflammation has subsided and the wound enters the remodeling phase. In this stage fibroblasts will degrade or produce collagen at a rate dependent on level of the collagen.

We further validated the model using data from (Madden and Peacock 1971) in which the amount of newly accumulated collagen and rate of accumulation in a wound were measured using 3–4 H^3 Proline to label the new collagen. Figure 8 shows that the scaled Madden and Peacock data agree with the simulated data in the model for an initial wound size of 0.6 ($WS_0 = 0.6$) with no pathogen present. Given that the variable in the model, *COL*, does not represent the exact level of collagen present, but rather a percentage of the wound covered, data presented in the work by Madden and Peacock were scaled by a single multiplier. The data from Madden and Peacock are scaled so that the end level for the collagen was slightly above one in the left panel. Additionally, the rates of accumulation data were scaled by the day 14 data (max). New collagen (*COL*) is zero in a new wound and one when the wound is healed. Values above one can occur during the healing process and are interpreted as scaring. Though the simulations do not match at every point, it can be seen that this model captures the overall dynamics of the wound healing process.

Using the validated model, the healing response to wounds with nonzero initial pathogen was simulated and is shown in Fig. 9. The dashed transients correspond to an initial pathogen load of $P_0 = 0.5$ in a small wound ($WS_0 = 0.6$) and the solid curves correspond to $P_0 = 1.5$ and $WS_0 = 0.6$. The higher initial pathogen level gives rise to a strong inflammatory response that thwarts the ability of the wound to heal, resulting in a chronic wound ($COL \ll 1$). The lower initial pathogen level gives rise to a larger inflammatory response than in the pathogen-free wound (Fig. 5), but the pro-inflammatory feedback is not sufficient to sustain the inflammation. Therefore, the wound is able to heal ($COL > 1$) and ultimately enters the remodeling stage.

Wounded tissue with a poor oxygen supply is known to have difficulty healing (London and Donnelly 2000). Given this sensitivity to the oxygen level at the wound

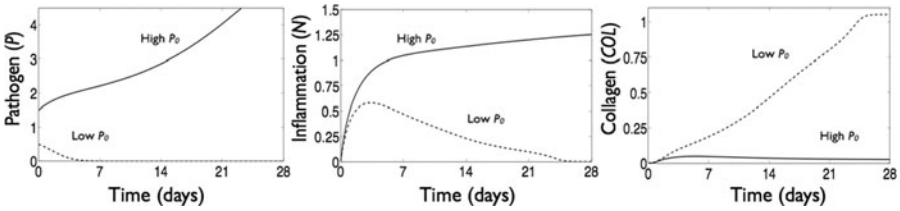

Fig. 9 Transient solutions of wound healing with high and low initial infection levels. *Solid line*—$P_0 = 1.5$ and *dashed line*—$P_0 = 0.5$. $WS_0 = 0.6$ and all other variables were initially set to background levels, $COL = 0$, $N = 0$, $FIB_p = 10$, $FIB_m = 0$, and $FIB_a = 0$

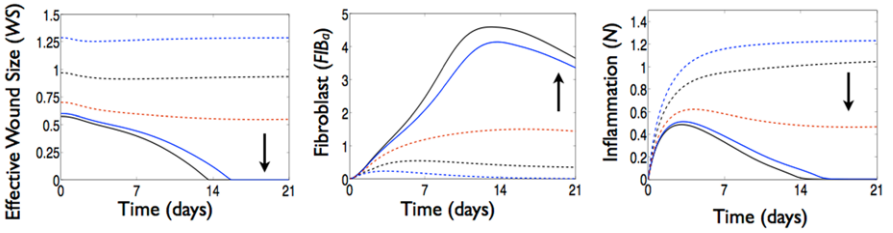

Fig. 10 Wound response to various O_2 levels. All transients have $WS_0 = 0.6$ and all other variables were initially set to background levels, $COL = 0$, $N = 0$, $FIB_p = 10$, $FIB_m = 0$, and $FIB_a = 0$. The *arrow* indicates the direction of increasing O_2 levels (10, 15, 20, 25, 30). *Solid curves* result in a healed wound. The *blue solid curve* has $O_2 = O_{crit} = 25$ and *black* $O_2 = 30$. The *dashed curves* result in a non-healed wound, *red* $O_2 = 20$, *black* $O_2 = 15$ and *blue* $O_2 = 10$ (Color figure online)

site, the model was used to predict wound healing dynamics for various oxygen levels. In Fig. 10, the effective wound size (WS), fibroblast (FIB_a), and inflammation (N) versus days since wounding were plotted for an initial wound size of 0.6 and with O_2 levels below, above and at O_{crit}. WS appears in the activation term of the inflammation equation, Eq. (13). When oxygen is reduced this term increases and results in additional activation of the inflammatory response despite the fact that the wound size has not actually increased. Dropping the O_2 levels below $O_{crit} = 25$ (blue solid curve) to 20 gives rise to an increase in WS and inflammation levels with decreases in fibroblast (red-dashed curves). New collagen is able to form in the wound. However, the wound does not fully heal; the effective wound size is nonzero at steady state. Further decreases lead to more significant changes in the transients, as seen with $O_2 = 15$ (black-dashed) and $O_2 = 10$ (blue-dashed). Healing is nearly fully suppressed, so the effective wound size remains very high. The fibroblasts are unable to mount an effective response and the wound is filled with inflammation. O_2 levels below 15.6 result in a non-healing wound with no new collagen.

Next the model was used to explore healing when oxygen is reduced and initial pathogen is nonzero. In Fig. 11 we present the transients for COL, FIB_a, N, WS, and P, with $P_0 = 0.7$, $O_2 = 22$, $WS_0 = 0.6$. This wound does not heal, even though the infection is eliminated after 8 days. The degradation of fibroblasts due to inflammation causes a drop in the fibroblast level. This resulting level of fibroblasts does not sustain collagen accumulation in the presence of inflammation, which continues to degrade the collagen resulting in a net loss. Lower collagen levels translate to larger effective

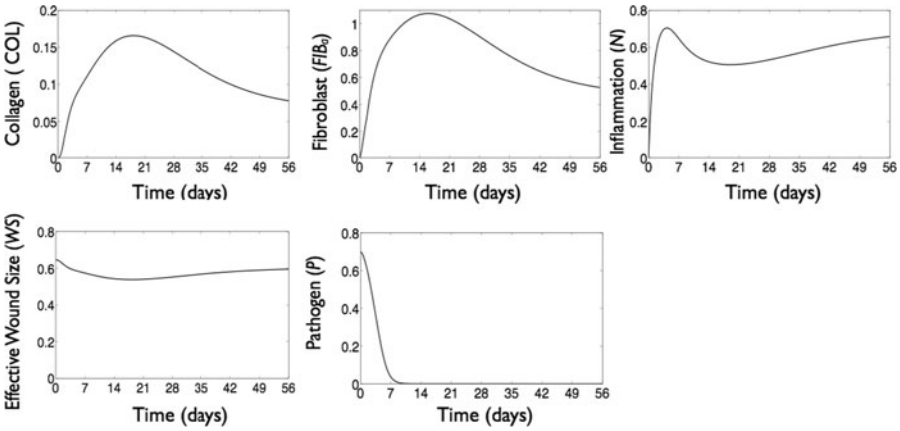

Fig. 11 Wound healing in an infected, oxygen depleted wound. Transients for collagen (*COL*), fibroblast (FIB_a), inflammation (N), effective wound size (WS) and pathogen (P) versus days of healing with $P_0 = 0.7$, $WS_0 = 0.6$, and $O_2 = 22$. All other variables were initially set to background levels, $COL = 0$, $N = 0$, $FIB_p = 10$, $FIB_m = 0$, and $FIB_a = 0$

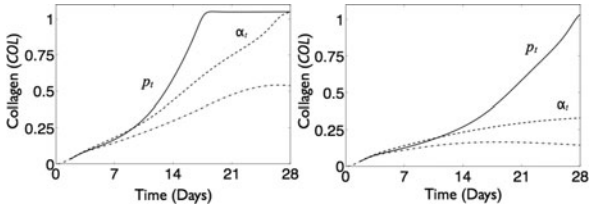

Fig. 12 Collagen accumulation in treated wounds with and without reduced O_2. *Left panel*, transients for collagen (*COL*) with normal healing (*dot-dashed*), antibiotic treatment (*dashed*, $\alpha_t = 10$), and altered fibroblast (*solid*, $p_t = 1.3$) with normal oxygen, $P_0 = 0.7$, and $WS_0 = 0.6$ and all other variables were initially set to background levels, $COL = 0$, $N = 0$, $FIB_p = 10$, $FIB_m = 0$, and $FIB_a = 0$. *Right panel*, all parameters and initial conditions are the same as the left panel except $O_2 = 20$. All treatments were implemented at $t = 2$ days

wound size and thus triggers further activation of inflammation around day 21, which qualitatively captures observed inflammation dynamics in a low O_2 environment as described in Eming et al. (2000).

Finally, the model is used to explore the use of treatment options in wound healing. Two treatment options were investigated: administering an antibiotic and altering fibroblast proliferation. A comparison of these treatment outcomes is shown in Fig. 12 in a normal wound ($O_2 = 25$, left panel) and a reduced O_2 level wound ($O_2 = 20$, right panel). The transients on the left correspond to a wound with normal O_2 levels. Antibiotic treated wounds are plotted with a dashed line, while the curves for increased proliferation of fibroblasts are plotted with a solid line.

To implement the treatment of antibiotics, the decay of pathogens was increased on day three by adding the term $-\alpha_t P$ to the pathogen equation. This change in decay was maintained for the remainder of the simulation. To alter the fibroblast proliferation, the proliferation rate of all fibroblasts was multiplied by p_t throughout the re-

mainder of the simulation. α_t and p_t are set so that they both result in a healed wound by week four, see Fig. 12a. In the non-treated wound (dot-dashed) with $P_0 = 0.7$ and $WS_0 = 0.6$ there is significant levels of new collagen but the wound does not heal, see Fig. 12a. When the wound is treated with antibiotics (dashed line) it takes the full four weeks to heal. When it is treated with altered fibroblast proliferation (solid line) the wound heals at approximately two and half weeks to heal. The simulations are then repeated in a wound with reduced tissue oxygenation ($O_2 = 20$), Fig. 12b. In a low oxygen environment, the untreated wound does not show significant healing. When antibiotic treatment is administered, the wound still does not heal, but there is increased collagen accumulation and the collagen levels remains at approximately 30 %. However, altering fibroblast activity was able to significantly change the outcome of the low oxygen wound. In the initial stage of healing the transients are similar for the normal and low O_2 environment. The antibiotic treatment is only effective while pathogen is present. Therefore, it is less effective at combating the low level of collagen during the latter stage of healing. While, the fibroblast treatment is effective throughout the healing process and brings about wound closure in the low O_2 environment.

4 Discussion

Mathematical models offer a non-invasive intermediary step between animal models and human subject studies that allow hypotheses and therapies to be tested prior to clinical studies. This is especially important for biological systems which consist of networks whose output is generally overlapping and nonlinear in the responses. An *in silico* model may increase the success rate of clinical trials and aid in designing more appropriate animal studies. These animal or clinical studies would then in turn, validate the model. *In silico* models allow the investigation of an integrated system as opposed to a reduced system, which by its very nature, has reduced complexity.

In this manuscript, a model of collagen accumulation as a marker of wound healing was developed. This system of ordinary differential equations tracks fibroblasts, collagen, inflammation and pathogens. The model was validated by comparison to the normal time course of wound healing by matching appropriate activity for the inflammatory, proliferative and remodeling phases. Subsequent validation was made by comparison to collagen accumulation experiments by (Madden and Peacock 1971). The model was then used to investigate the impact of local oxygen levels on wound healing and to confirm that oxygen plays an important role in successful wound healing. Finally, a comparison of two wound healing therapies, antibiotics and increased fibroblast proliferation, was presented.

The present study represents only a step towards the development of a detailed mathematical model of acute wound healing. Consequently, there are many opportunities for improving upon this existing model; for example:

- No attempt was made for an exhaustive study of the impact of individual parameters on long-term healing behavior. It was found previously (Menke et al. 2010), and confirmed here, that the fibroblast proliferation rate can improve wound healing and it is likely that other parameters have a profound impact on healing as well.

- This model development focused on strongly interlinked local factors (inflammation, fibroblast function and recruitment, formation of collagen, bacterial contamination, and tissue oxygenation) with resultant dynamic nonlinear behavior. Factors such as depth and shape of the wound, wound contraction, epithelization, and angiogenesis have not been addressed.
- Currently, the model uses a fixed level for oxygen. This can be used to represent an underlying vascular disease state (such as in a diabetic patients). Because local oxygen levels change as a result of a wound and over the course of wound healing, modeling the dynamic oxygen level could be useful.
- In addition, systemic effects on wound healing, e.g., nutritional status, age, sex, and underlying co-morbidities were not included.

This model demonstrates the use of a systems biology approach to human wound healing. A refined method of computational analysis would decrease overall cost, time, and need for invasive testing. We are optimistic that including systemic effects will enhance our understanding of the acute wound healing process and ultimately lead to improved clinical therapies.

References

Almeida, L., Bagnerini, P., Habbal, A., Noselli, S., & Serman, F. (2011). A mathematical model for dorsal closure. *J. Theor. Biol.*, *268*(1), 105–119. doi:10.1016/j.jtbi.2010.09.029.

Ballard, J. L., Eke, C. C., Bunt, T. J., & Killeen, J. D. (1995). A prospective evaluation of transcutaneous oxygen measurements in the management of diabetic foot problems. *Vasc. Surg.*, *22*, 485–490.

Buckley, C. D., Pilling, D., Lord, J. M., Akbar, A. N., Scheel-Toellner, D., & Salmon, M. (2001). Fibroblasts regulate the switch from acute resolving to chronic persistent inflammation. *Trends Immunol.*, *22*(4), 199–204.

Caselli, A., Latini, V., Lapenna, A., Di Carlo, S., Pirozzi, F., Benvenuto, A., & Uccioli, L. (2005). Transcutaneous oxygen tension monitoring after successful revascularization in diabetic patients with ischaemic foot ulcers. *Diabet. Med., J. Br. Diabet. Assoc.*, *22*(4), 460–465. doi:10.1111/j.1464-5491.2005.01446.x.

Diegelmann, R. F., & Evans, M. C. (2004). Wound healing: an overview of acute, fibrotic and delayed healing. *Front. Biosci.*, *9*(1–3), 283. doi:10.2741/1184.

Eming, S. A., Krieg, T., & Davidson, J. M. (2000). Inflammation in wound repair: molecular and cellular mechanisms. *J. Invest. Dermatol.*, *127*(3), 514–525.

Flegg, J. A., Byrne, H. M., & McElwain, L. S. (2010). Mathematical model of hyperbaric oxygen therapy applied to chronic diabetic wounds. *Bull. Math. Biol.*, *72*(7), 1867–1891. doi:10.1007/s11538-010-9514-7.

Friedman, A., Hu, B., & Xue, C. (2010). Analysis of a mathematical model of ischemic cutaneous wounds. *SIAM J. Math. Anal.*, *42*(5), 2013–2040. doi:10.1137/090772630.

Goldberg, S. R., & Diegelmann, R. F. (2010). Wound healing primer. *Surg. Clin. North Am.*, *90*(6), 1133–1146. doi:10.1016/j.suc.2010.08.003.

Greenhalgh, D. G. (1998). The role of apoptosis in wound healing. *Int. J. Biochem. Cell Biol.*, *30*(9), 1019–1030. doi:10.1016/S1357-2725(98)00058-2.

Grinnell (1994). Fibroblasts, myofibroblasts, and wound contraction. *J. Cell Biol.*, *124*(4), 401–404.

Harley, C. B., Futcher, A. B., & Greider, C. W. (1990). Telomeres shorten during ageing of human fibroblasts. *Nature*, *345*(6274), 458–460. doi:10.1038/345458a0.

Javierre, E., Vermolen, F. J., Vuik, C., & van der Zwaag, S. (2009). A mathematical analysis of physiological and morphological aspects of wound closure. *J. Math. Biol.*, *59*(5), 605–630. doi:10.1007/s00285-008-0242-7.

Kuehn, B. M. (2007). Chronic wound care guidelines issued. *JAMA J. Am. Med. Assoc.*, *297*(9), 938–939. doi:10.1001/jama.297.9.938.

Kühne, H. H., Ullmann, U., & Kühne, F. W. (1985). New aspects on the pathophysiology of wound infection and wound healing—the problem of lowered oxygen pressure in the tissue. *Infection*, *13*(2), 52–56.

London, N. J. M., & Donnelly, R. (2000). Ulcerated lower limb. *Br. Med. J.*, *320*(7249), 1589–1591. doi:10.1136/bmj.320.7249.1589.

Madden, J. W., & Peacock, E. E. (1971). Studies on the biology of collagen during wound healing, 3: dynamic metabolism of scar collagen and remodeling of dermal wounds. *Ann. Surg.*, *174*(3), 511–520.

Martin, P., & Leibovich, S. J. (2005). Inflammatory cells during wound repair: the good, the bad and the ugly. *Trends Cell Biol.*, *15*(11), 599–607. doi:10.1016/j.tcb.2005.09.002.

Menke, N. B., Cain, J. W., Reynolds, A., Chan, D. M., Segal, R. A., Witten, T. M., Bonchev, D. G., Diegelmann, R. F., & Ward, K. R. (2010). An in silico approach to the analysis of acute wound healing. *Wound Repair Regen.*, *18*(1), 105–113. doi:10.1111/j.1524-475X.2009.00549.x.

Menke, N. B., Ward, K. R., Witten, T. M., Bonchev, D. G., & January, R. F. D. (2006) Impaired wound healing. *Clin. Dermatol.*, *25*(1), 19–25. doi:10.1016/j.clindermatol.2006.12.005.

Paulsen, F., Pufe, T., Conradi, L., Varoga, D., Tsokos, M., Papendieck, J., & Petersen, W. (2002). Antimicrobial peptides are expressed and produced in healthy and inflamed human synovial membranes. *J. Pathol.*, *198*(3), 369–377. doi:10.1002/path.1224.

Raj, P. A., & Dentino, A. R. (2002). Current status of defensing and their role in innate and adaptive immunity. *FEMS Microbiol. Lett.*, *206*(1), 9–18. 2. doi:10.1016/S0378-1097(01)00496-7.

Reynolds, A., Rubin, J., Clermont, G., Day, J., & Ermentrout, G. B. (2006). A reduced mathematical model of the acute inflammatory, I: derivation of model and analysis of anti-inflammation. *J. Theor. Biol.*, *242*(1), 220–236. doi:10.1016/j.jtbi.2006.02.016.

Ross, R. (1968). The fibroblast and wound repair. *Biol. Rev.*, *43*(1), 51–91. doi:10.1111/j.1469-185X.1968.tb01109.x.

Schilling, J. A. (1968). Wound healing. *Physiol. Rev.*, *48*(2), 374–423.

Sherratt, J. A., & Dallon, J. C. (2002). Theoretical models of wound healing: past successes and future challenges. *C. R. Biol.*, *325*(5), 557–567.

Smith, R. S., Smith, T. J., Blieden, T. M., & Phipps, R. P. (1997). Fibroblasts as sentinel cells. Synthesis of chemokines and regulation of inflammation. *Am. J. Pathol.*, *151*(2), 317–322.

Stefanini, M. O., Th Wu, F., Gabhann, F. M., & Popel, A. S. (2008). A compartment model of VEGF distribution in blood, healthy and diseased tissues. *BMC Syst. Biol.*, *2*, 19. doi:10.1186/1752-0509-2-77.

Takai, Y., Miyoshi, J., Ikeda, W., & Ogita, H. (2008). Nectins and nectin-like molecules: roles in contact inhibition of cell movement and proliferation. *Nat. Rev. Mol. Cell Biol.*, *9*(8), 603–615. doi:10.1038/nrm2457.

Turner, L., Scotton, C., Negus, R., & Balkwill, F. (1999). Hypoxia inhibits macrophage migration. *Eur. J. Immunol.*, *29*, 2280–2287.